GeroScience
https://doi.org/10.1007/s11357-024-01340-8

ORIGINAL ARTICLE

Fixel-based and tensor-derived white matter abnormalities in relation to memory impairment and neurocognitive disorders

Charly Hugo Alexandre Billaud · Junhong Yu · for the Alzheimer's Disease Neuroimaging Initiative

Received: 22 March 2024 / Accepted: 5 September 2024

Abstract Aging-related neurocognitive disorders, including Alzheimer's disease (AD) and mild cognitive impairment (MCI), have been characterised by altered brain white matter (WM), relying widely on diffusion tensor imaging (DTI). DTI's limited accuracy in assessing crossing fibres prompted novel methods that distinguish fibres crossing through same voxel-spaces, such as fixel-based analysis (FBA), highlighting subtle macrostructural and microstructural alterations in AD and MCI. We examined the FBA and DTI's specificity in determining WM features relevant to memory in the neurocognitive aging spectrum. Diffusion-weighted images were analysed in 560 participants with various neurocognitive diagnoses from the Alzheimer's Disease Neuroimaging Initiative (F:297; mean age: 73.2 ± 8). Verbal memory was measured in 488 participants using the Rey Auditory Verbal Learning Test. FBA-derived measures of fibre density (FD), fibre-bundle cross-section (FC), and their combination (FDC), DTI fractional anisotropy (FA) and mean diffusivity (MD) were examined in relation to diagnoses and memory scores, controlling for age, sex, and intracranial volume. MCI and AD groups significantly differed from controls, with lower FD and FDC in the fornix and bilateral fibres extending to the medial temporal lobes (MTL). Memory was positively associated with FD and FDC in the fornix and MTL fibres, and FC in the anterior commissure (AC). Widespread FA reductions and MD increases were observed in AD and MCI and widely associated with memory. Fixel-wise measures highlight fibre tracts that are altered distinctly at the macroscopic and microscopic level in neurocognitive aging, and reveals structures associated with memory performance that are more specifically located than tensor-derived measures.

Keywords Fixel-based · White matter · Alzheimer's · Mild cognitive impairment · Memory · Aging

Key points
- Fixel-based metrics were reduced in the fornix and the medial temporal lobe in AD and MCI.
- Fixel-based reductions are related to worse memory performance.
- Fixel-wise metrics give better anatomical specificity than tensor-derived measures.

Data used in preparation of this article were obtained from the Alzheimer's Disease Neuroimaging Initiative (ADNI) database (adni.loni.usc.edu). As such, the investigators within the ADNI contributed to the design and implementation of ADNI and/or provided data but did not participate in analysis or writing of this report. A complete listing of ADNI investigators can be found at: http://adni.loni.usc.edu/wpcontent/uploads/how_to_apply/ADNI_Acknowledgement_List.pdf.

C. H. A. Billaud (✉) · J. Yu
School of Social Sciences, Nanyang Technological University, 48 Nanyang Avenue, PsychologySingapore 639798, Singapore
e-mail: charly.billaud@ntu.edu.sg

J. Yu
e-mail: junhong.yu@ntu.edu.sg

Published online: 13 September 2024

Introduction

Cerebral white matter (WM) is known to be altered in age-related neurocognitive disorders, including individuals with Alzheimer's disease (AD) as well as mild cognitive impairment (MCI) [1, 2]. Studies of WM have widely relied on diffusion weighted magnetic resonance imaging (MRI) a non-invasive method able to measure the motion of water molecules in the brain tissues; and in turn assess the microstructural integrity of WM fibres (diffusion tensor imaging, DTI) [3].

DTI approach has been recognised to lack accuracy and reliability within image voxels containing multiple crossing fibres in different directions, which is estimated to represent up to 90% of WM voxels [4, 5]. To this end, the "fixel-based" analyses approach was recently conceived to focus on *fixels*, i.e., specific fibre populations within voxels, and allows to identify and describe multiple crossing fibres contained inside a voxel [6, 7] without averaging the voxel's content indiscriminately [4]. In fixel-based analyses (FBA), the "connectivity" of a given fixel, i.e., its ability to transmit information, can be measured by: the apparent fibre density (referred here as FD), estimated from the radial water diffusion approximately proportional to the intra-axonal volume [8], which reflects microstructural alterations; the fibre-bundle cross-section (FC), estimating the macrostructural alteration of the fibre bundle along the fixel's orientation; and a metric combination of both independent measures (FDC) [6, 7]. These measures were used to highlight WM atrophy in specific tracts in neurocognitive disorders such as AD and MCI [5, 9, 10], and were able to shed light on altered fibres in WM voxels defined unaffected in a conventional DTI voxel-averaging [5].

In AD, decreases in FC, reflecting macroscopic degeneration, and decreases in FD, reflecting microscopic degeneration, have been observed in various tracts including the corpus callosum (CC), splenium and genu, arcuate fasciculus, superior/inferior longitudinal fasciculus, uncinate fasciculus, dorsal/ventral cingulum, inferior frontal-occipital fasciculus, posterior thalamic radiation, column and body of the fornix [5, 9–13]. In one AD study, FC decrease was associated with whole-brain volume atrophy [12], which suggests AD neurodegeneration is tied to macroscopic WM alterations. FBA in MCI also highlighted decreases in FDC affecting the posterior cingulum, the right uncinate fasciculus [5] and reduced FD and FC affecting the cingulum, uncinate fasciculus, anterior thalamic radiation, and forceps minor [14].

Fixel-wise microstructural and macrostructural features may be related to cognitive performance in neurocognitive aging, but few have investigated neuropsychological measures. Most studies including AD and MCI so far have only looked at measures of disease severity such as the mini-mental state examination (MMSE) or the clinical dementia rating (CDR), which have been associated with conventional voxel-wise measures with DTI [1], and also with FC and FD alterations in the CC, the fornix, posterior thalamic radiation, bilateral dorsal cingulum fasciculus/inferior frontal-occipital fasciculus [10, 13], which suggests these features of WM anatomy may be tied to neurocognitive decline. In typical aging, FD in the cerebello-thalamo-striatal tract and the fornix (but not FC) has been found to decrease with age [15, 16] and the fornix FD was correlated with worse memory performance in RAVLT's delayed recall [15]. One MCI study to date has verified an association between decreased FBA metrics in tau-associated tracts (parahippocampal segment of the cingulum and inferior longitudinal fasciculus) and worse memory performance in a ten-word delayed recall test [14].

To expand the current scientific literature and help determine fibres relevant to cognitive decline across the neurocognitive aging spectrum, we aimed at investigating whole-brain fixel-wise measures in the neurocognitive aging spectrum, comparing cognitively normal (CN) aging individuals to individuals with AD, MCI, and subjective memory complaint (SMC). Another objective was to assess the overall association of fixel-wise and memory performance. To supplement the FBA analysis, we have also included a similar conventional whole-brain TBSS analysis to test FA and MD across groups and in relation to memory. We tested the hypotheses that FD, FDC, FC, and FA are decreased, and that MD is increased in AD, MCI, and SMC compared to cognitively normal aging individuals, particularly in the fornix and the hippocampal formation, and that patterns of decreases are associated with lower memory performance in the neurocognitive aging spectrum.

Materials and methods

Participants

A dataset of participants was obtained from the Alzheimer's Disease Neuroimaging Initiative (ADNI, adni.loni.usc.edu). The ADNI is a partnership started in 2003 under the direction of Michael W. Weiner, MD, to investigate the combination of serial MRI, positron emission tomography (PET), other biological markers, as well as clinical and neuropsychological assessment to measure the progression of MCI and early AD (see www.adni-info.org for complete and up-to-date information). Details regarding the criteria for dementia and MCI used in the ADNI are available at https://adni.loni.usc.edu/wp-content/uploads/2008/07/adni2-procedures-manual.pdf. Ethical approval for the ADNI study was obtained by the ADNI investigators.

Participants from the ADNI-3 database [17] were selected across the neurocognitive aging spectrum (cognitively normal, with subjective memory complaints, and meeting diagnostic criteria for MCI and AD) to maximize variability in the cognitive and neuroimaging measures. Inclusion criteria required a valid T1 MPRAGE, 'ADNI-3 Basic' diffusion scans. Participants who were scanned only with the 'ADNI-3 Advanced' diffusion protocol were not included due to incompatibility in the protocols. In the sample, participants who had completed the *Rey Auditory Verbal Learning Test* (RAVLT) were selected.

Demographics information on the sample is summarised in Table 1. The participants' age ranged from 55.1 to 95.4 years. 79 participants out of the 560 participants were under 65 years of age (5 AD, 32 MCI, 1 SMC, and 41 CN). Across participants who completed the RAVLT, no significant difference in age across groups was observed ($F(\text{df}) = 0.665$ (3), $p = 0.574$). There was a significant difference in sex distribution in the sample (X^2 (df) = 10.372 (3), $p = 0.016$), with "cognitively normal" controls having significantly higher proportion of female participants compared to the other groups (adjusted standardised residual = 2.9).

Neuropsychological tests

The RAVLT completed by the aforementioned subgroup of 488 participants is a validated measure of declarative memory [18]. In the RAVLT, each participant is given a list (list A) of 15 unrelated words to learn and recall immediately aloud over five trials (Immediate recall test). Each is then given an interference list (list B) of 15 unrelated words once, to learn and immediately recall; after that the participant is required to recall aloud list A's words. After a 30 min delay, each is asked again to recall list A's words (30-min delay recall). Finally, a 50 words list is given to each participant, including words from list A and B, and 20 new distractor words, from which each had to identify words of list A (Recognition).

Neuroimaging acquisition

The neuroimaging acquisition protocol is summarised in Table 2. ADNI3 data varied across scanners and protocols (https://adni.loni.usc.edu/), with $b = 1000$ s/mm2 volumes in 16 to 55 directions (mean = 44.5), and 1 to 7 $b = 0$ s/mm^2 values (mean = 4.3) per DWI scan.

Table 1 Demographic characteristics of the sample

	Total	CN	MCI	SMC	AD
Overall sample	$N = 560$	$N = 288$	$N = 211$	$N = 22$	$N = 39$
Age in years (m ± sd)	73.2 ± 8	72.6 ± 8	73.6 ± 8	75.6 ± 5	74 ± 8
Sex F:M	297:263	175:113	98:113	11:11	13:26
MMSE (m ± sd)	27.8 ± 3[a]	29 ± 1[a]	27 ± 3[a]	29 ± 1	22.5 ± 3
Education years (m ± sd)	16.4 ± 2	16.6 ± 2	16.2 ± 3	16.4 ± 2	15.6 ± 2
Completed the RAVLT	$N = 488$	$N = 257$	$N = 180$	$N = 22$	$N = 29$
Age in years (m ± sd)	73.3 ± 8	73.1 ± 8	73.4 ± 8	75.6 ± 5	73.5 ± 8
Sex F:M	258:230	152:105	85:95	11:11	10:19
MMSE (m ± sd)	27.8 ± 3[a]	29 ± 1[a]	26.9 ± 4[a]	29 ± 1	22.1 ± 3
Education years (m ± sd)	16.4 ± 2	16.7 ± 2	16 ± 3	16.4 ± 2	15.6 ± 2

AD, Alzheimer's disease; *MCI*, mild cognitive impairment; *SMC*, subjective memory complaint; *CN*, cognitively normal; *MMSE*, mini-mental state examination; *RAVLT*, Rey Auditory Verbal Learning Test

[a]2 scores missing, 1 MCI and 1 CN

Table 2 Neuroimaging protocol

Sequence	Dimensions (mm)	Parameters	Time
T1 (Accelerated Sagittal MPRAGE)	208 × 240x256	TE = min full echo TR = 2300 TI = 900	6:20
Diffusion weighted	232 × 232x160	TE = 56; TR = 7200; single-shell b = 1000 s/mm^2	7:30

Refer to ADNI3 (https://adni.loni.usc.edu/) for complete information on MRI protocols:

https://adni.loni.usc.edu/wp-content/themes/freshnews-dev-v2/documents/mri/ADNI3_MRI_Analysis_Manual_20180202.pdf

Diffusion weighted imaging preprocessing

The diffusion weighted images (DWI) were preprocessed using MRTrix v3.0.4 (https://www.mrtrix.org/) [7, 19, 20]. MP-PCA denoising was done on the diffusion weighted images [21], with Gibbs-ringing artifact removal [22], distortion correction, and N3 bias field correction [23].

For the FBA analysis, the Dhollander algorithm [24] was used to estimate the average response function of WM, grey matter (GM), and cerebrospinal fluid (CSF) from the bias corrected images, and the images upsampled to 1.25 mm in isotropic voxel size. Multi-shell multi-tissue constrained spherical deconvolution was applied to estimate fibre orientation distribution (FOD) from the WM and CSF response functions (which works on single-shell data with $b=0$ and $b=1000$ values) [25], and normalised with the *mtnormalise* command.

In line with previous FBA studies [5, 10], a study-specific FOD template was generated based on a representative subset of 40 random participants including 10 CN, 10 MCI, 10 SMC, 10 AD; each group with 5 females and 5 males, and a similar age distribution as the whole sample (Kolmogorov–Smirnov at $p>0.05$). Each participant FOD was registered to the study FOD template. A template whole brain mask was generated to establish where fixels were to be measured and the cerebellum was manually removed in freeview tool in Freesurfer [26]. A fixel mask was defined from the FOD template using connectivity-based fixel enhancement [27] and manually visualised to check for inclusion of fixels within WM and not GM (-fmls_peak_value set at 0.15 in this dataset), resulting in a mask of 291685 fixels (Fig. 1).

Participant's individual fixels were matched to the fixel mask to obtain a fixel-fixel correspondence. Based on the defined fixels, the apparent fibre density (FD), log of fibre-bundle cross-section (log(FC)) and the combination of fibre density and cross-section (FDC) measures were computed in each participant [6]. A whole-brain fibre tractogram of 20 million streamlines was generated based on the FOD template at amplitude cut-off 0.15, reduced to 2 million fibres using the Spherical-deconvolution informed filtering of tractograms (SIFT) algorithm [28]. Based on that tractogram, fixel-fixel connectivity matrices for each measure were generated and used to smooth the fixel values across connected fixel neighbours (at 10 mm fixelfilter command).

For the DTI analysis, diffusion tensors were created from the corrected DWI in MRTRIX, from which fractional anisotropy (FA) and mean diffusivity (MD) metrics were extracted across WM voxels. The FA data was analysed with the Tract-Based

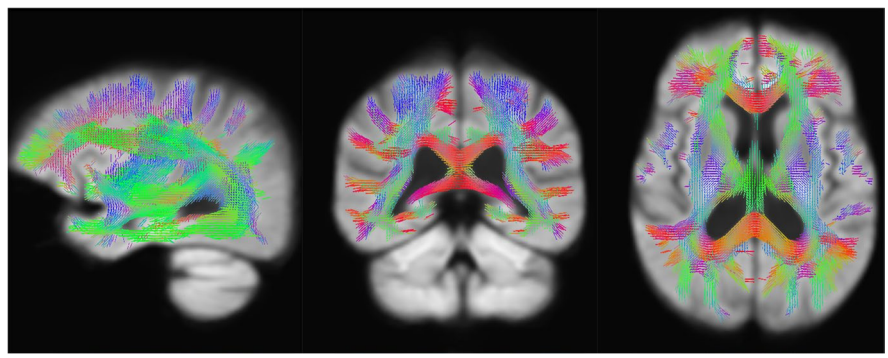

Fig. 1 Fixel mask overlaid on the white matter fibre orientation distribution template. *Note*. Displayed using mrview tool in MRTRIX3 [20]

Spatial Statistics (TBSS) tool [29] from the FMRIB Software Library [30]. Using TBSS, the FA and MD data were aligned across participants and registered to the FMRIB58_FA template (which is in 1 × 1x1mm MNI152 standard space). This allowed to estimate a mean "skeleton" (representing centre of all tracts in the sample) was built. The cerebellum was masked out, with the fsleyes tool in FSL using the MNI structural atlas (References: https://fsl.fmrib.ox.ac.uk/fsl/fslwiki/Atlases). Individual data was projected to this common skeleton for statistical analyses, in two skeletons separately (FD and MD).

Statistics

A composite memory score was developed from the Learning, Immediate, 30-min delay recall, and Recognition scores in the RAVLT, with a confirmatory factor analysis (CFA) defining the composite score as one latent variable explained by the four scores. The CFA was computed with the *lavaan* package [31] in R *v*4.3.2 [32], with the maximum likelihood ratio estimation (estimator = "MLR", missing = "ML") options and the lavPredict function to obtain the latent variable values (Rosseel, 2012). The composite score was normalised on a scale from 0 to 1.

Connectivity-based fixel enhancement (CFE), which uses information from the tractography to estimate threshold-free test-statistics across bundles of fixels estimated to be structurally connected [27], was applied to test linear models predicting FBA measures in individual fixels. Whole-brain fixel-wise estimates of FD, log(FC), and FDC were included as dependent variables in separate general linear models. The control group's fixel-wise measures (FD, log(FC), and FDC) were first compared against each clinical group separately, including all 560 participants. To investigate memory's association FBA, three models were tested including the subgroup ($N = 488$) having completed the RAVLT. The models tested for the two-sided association of each fixel-wise measure with the memory composite score, controlling for age and sex. The log of intracranial volume (log(ICV)), was also controlled in models predicting FC and FDC, as supported by previous findings of ICV influencing these two measures and its log being most appropriate [33]. ICV was estimated using mri_segstats in Freesurfer as part of the processing pipeline [26, 34]. The control variables were also normalised on a scale from 0 to 1 to avoid rank deficiency and poor design matrix conditioning. CFE was run with 5000 permutations and the results corrected for family-wise error (FWE) at $p = 0.05$.

Group differences and association with memory were also investigated with DTI FA and MD metrics using FSL's *randomise* permutation tool [35]. The FA and MD values were separately fit into two-sided general linear models with 5000 permutations and threshold-free cluster enhancement, testing for FA and MD respective differences between the AD, SMC, MCI groups compared to CN participants, and FA and MD's association with the memory composite score, all controlling for age, sex and estimated ICV; FWE-corrected at $p = 0.05$.

Results

Neuropsychological assessment

Figure 2 describes scores of the selected RAVLT subtests and the estimated composite score across groups. Six individual scores were missing for the RAVLT learning task: 3 MCI and 3 AD. The composite score accounted for the missing data as described in the statistics section. The SMC group was not significantly different from the CN group in all assessed memory scores (all *t*-tests $p > 0.12$), whilst those with MCI and AD score significantly worse in all memory scores (all *t*-tests $p < 0.001$, Cohen's $d < -0.76$), with the AD group performing the worse.

The CFA used to estimate the memory composite score had a good model fit ($X^2 = 4.104$; CFI = 0.998; RMSEA = 0.046 [90% CI = < 0.001–0.111]; SRMR = 0.011). The beta and standardised beta coefficients for each measure are depicted in Fig. 3.

Fixel-based analysis examining diagnostic group differences

The AD group did not have a significant increase in FD and FDC compared to controls. Significantly lower FD in the fornix and bilateral fibres extending to the medial temporal lobes (MTL); as well as fibres posterior to the thalamus longing the anterior curve of the lateral ventricles (Fig. 4a). Significantly reduced FDC had both the patterns from the fornix to the MTL, as well as fibres from the anterior

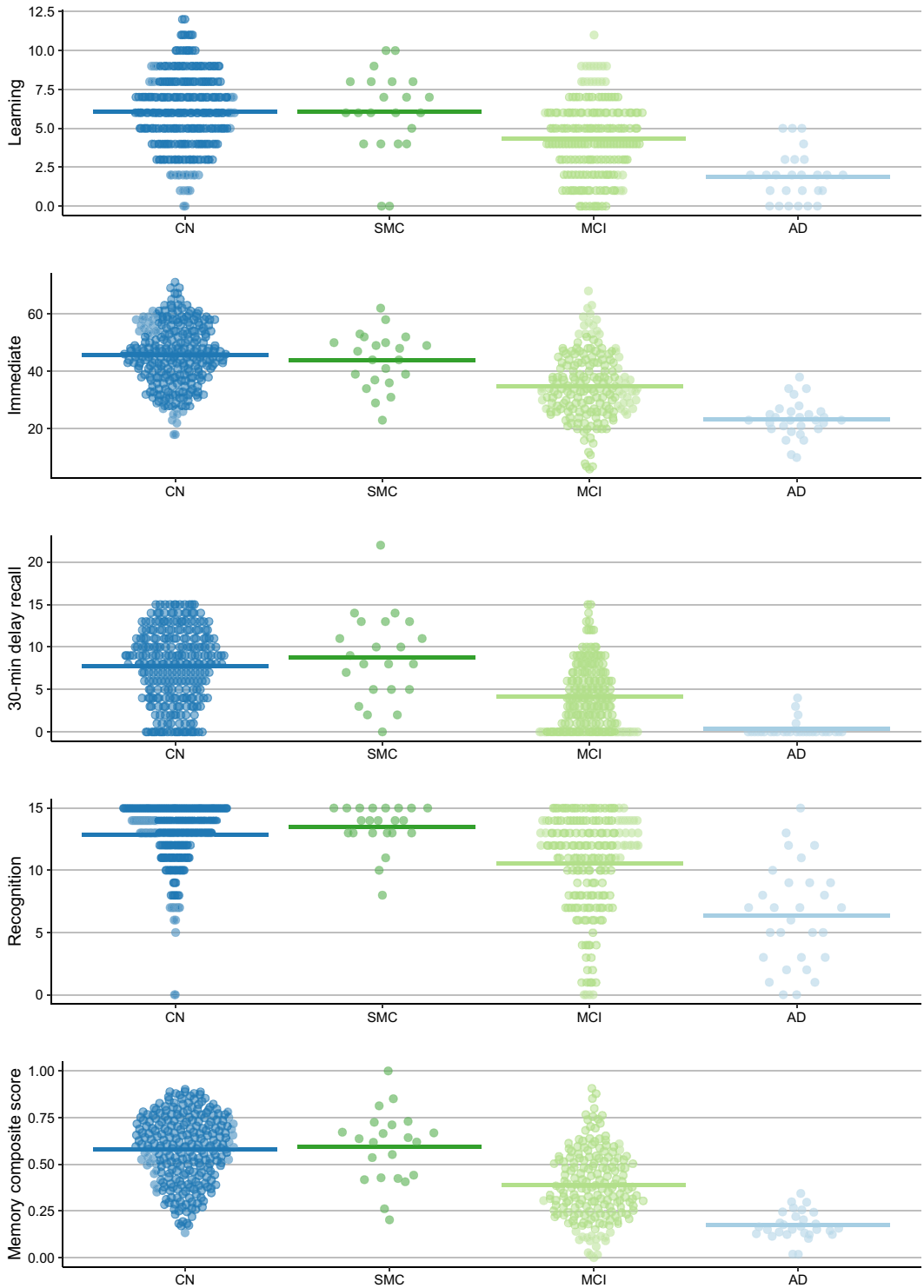

Fig. 2 Scores from selected subtests of the Rey Auditory Verbal Learning Test. *Note*. AD, Alzheimer's disease; MCI, mild cognitive impairment; SMC, subjective memory complaint; CN, cognitively normal

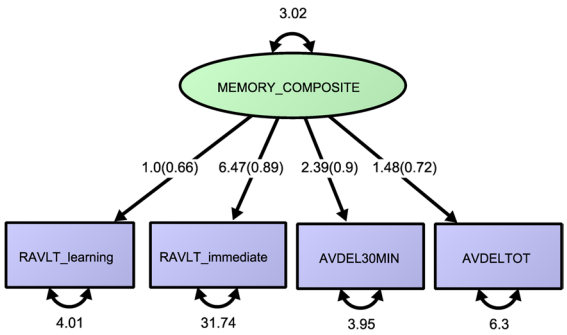

Fig. 3 Confirmatory factor analysis (CFA) estimating the memory composite score. *Note*. Plotted using the R package 'onyxR' [36]. AVDEL30MIN, 30-min delay recall; AVDELTOT, recognition

commissure (AC), especially in its left anterior part (Fig. 4b). Log(FC) was significantly lower in the left part of the AC, but significantly higher in the fornix (extending down the left hemisphere) and in fibres along the septum pellucidum (Fig. 4c).

No significant increase in FD, FDC, or log(FC) was observed in the MCI group compared to controls. In comparison to controls, MCI FD was decreased in the fornix, with fibres extending down the MTL bilaterally, layers of fibres longing the curve of lateral ventricles both anterior and posterior to it (longing the posterior horn, within tracts from splenium of the CC), and few sparse fibres in the AC and right tract from the anterior midbody of the CC (Fig. 4d). FDC was significantly decreased specifically in the bilateral columns of the fornix and fibres extending down the MTL, the anterior midbody of the CC, and the superior longitudinal fasciculi, especially right (Fig. 4e). Log(FC) was significantly decreased in parts of the bilateral cortico-spinal tracts, mostly in the left tract and isolated to the pontine levels in the left (Fig. 4f). No significant difference in FD, FDC, or log(FC) was observed between the SMC group and controls.

Fixel-based analysis examining associations between fixel-based metrics and memory

The whole-brain fixel based analysis shows that FD was significantly associated with memory mainly in WM fibres in the fornix, with fibres extending bilaterally down the MTL. Significant fixels longing the anterior and posterior surface of the lateral ventricles are also visible. A few fibres were also significant in the left top part of the AC tract ($p_{FWE} < 0.05$) (Fig. 4g). FDC had similar associations to FD, affecting the fornix, extending down in the MTLs (Fig. 4h), with although with less fixels along the lateral ventricles. Log(FC) was positively associated with the memory score in fixels of the AC tract especially the anterior parts of the tract leading to the bilateral temporal poles (Fig. 4i). No significant negative association with memory was detected for any of the FBA measures. Table 3 describes the FBA values of the positive significant fixels.

TBSS analyses examining diagnostic group differences

In AD, there was no significant increase in FA or decrease in MD compared to controls. Decreased FA and increased MD were found bilaterally in the cingulum bundle (less in the anterior part for MD), the CC (except anterior midbody), fornix, inferior longitudinal fasciculi, the striato-parietal and occipital radiations (Fig. 5a).

In the MCI group, there were no significant increase in FA or reductions in MD compared to controls. Widespread FA decreases were found, mostly not significant in the bilateral internal capsules, superior corona radiatae, and parts of the superior longitudinal fasciculi. Widespread MD increases were detected bilaterally in the posterior/temporal part of the cingulum bundle, the CC (except splenium), fornix, inferior longitudinal fasciculi, the striato-parietal radiations (Fig. 5b). For the SMC group, there were no significant differences in MD and FA compared to controls.

TBSS analyses examining associations between FA, MD, and memory

Figure 5c, shows widespread clusters of FA decrease and MD increases in the WM skeleton that are significantly associated with lower memory scores. Of note, there appears to be an absence of significant MD clusters in the anterior and posterior limbs of the bilateral internal capsule and right external capsule, as well as in superior ends of the stratio-precentral and prefrontal tracts, and an absence of FA clusters in the bilateral internal capsules, as well as the bilateral superior corona radiatae.

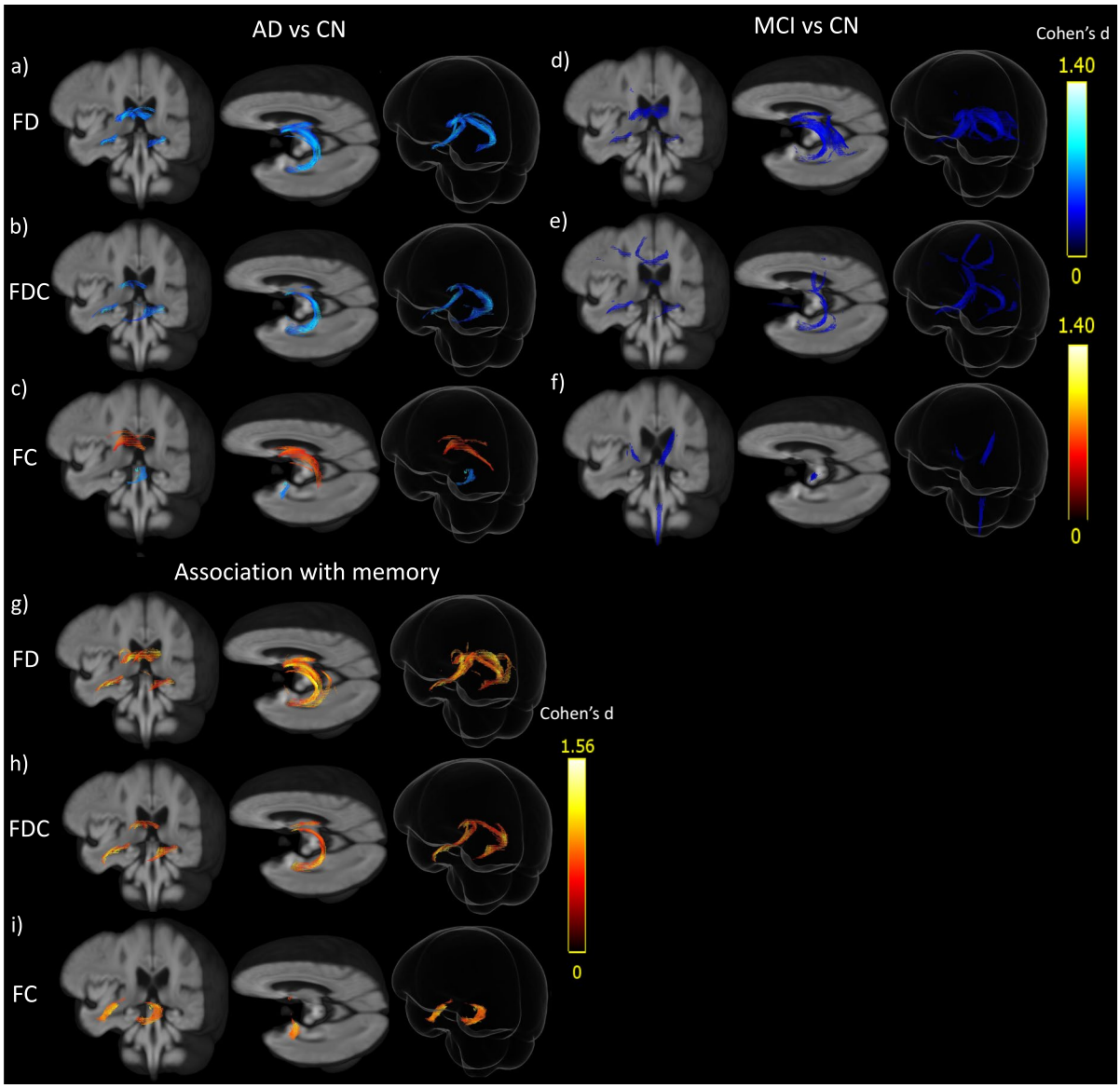

Fig. 4 Fixel-based measures compared across controls and clinical subgroups and associated with memory. *Note*. Fixels where effect is significant at $p_{FWE} < .05$. AD, Alzheimer's disease; CN, Cognitively normal; FD, fibre density; FDC, combined measure of FD and FC; FC, fibre-bundle cross-section. Red to yellow scales is an increase compared to controls and blue to white a decrease

Table 3 Fixel-based descriptive stats of the significant fixels

FBA measure	Mean	Median	std	Min	Max	*N* fixels
FD	0.369653	0.346557	0.0818554	0.236804	0.714309	2658
FDC	0.37872	0.355679	0.110717	0.21183	0.776455	1391
Log(FC)	0.149354	0.137423	0.0641479	0.0297263	0.279751	930

FD, fibre density; *FDC*, combined measure of FD and FC; *FC*, fibre-bundle cross-section

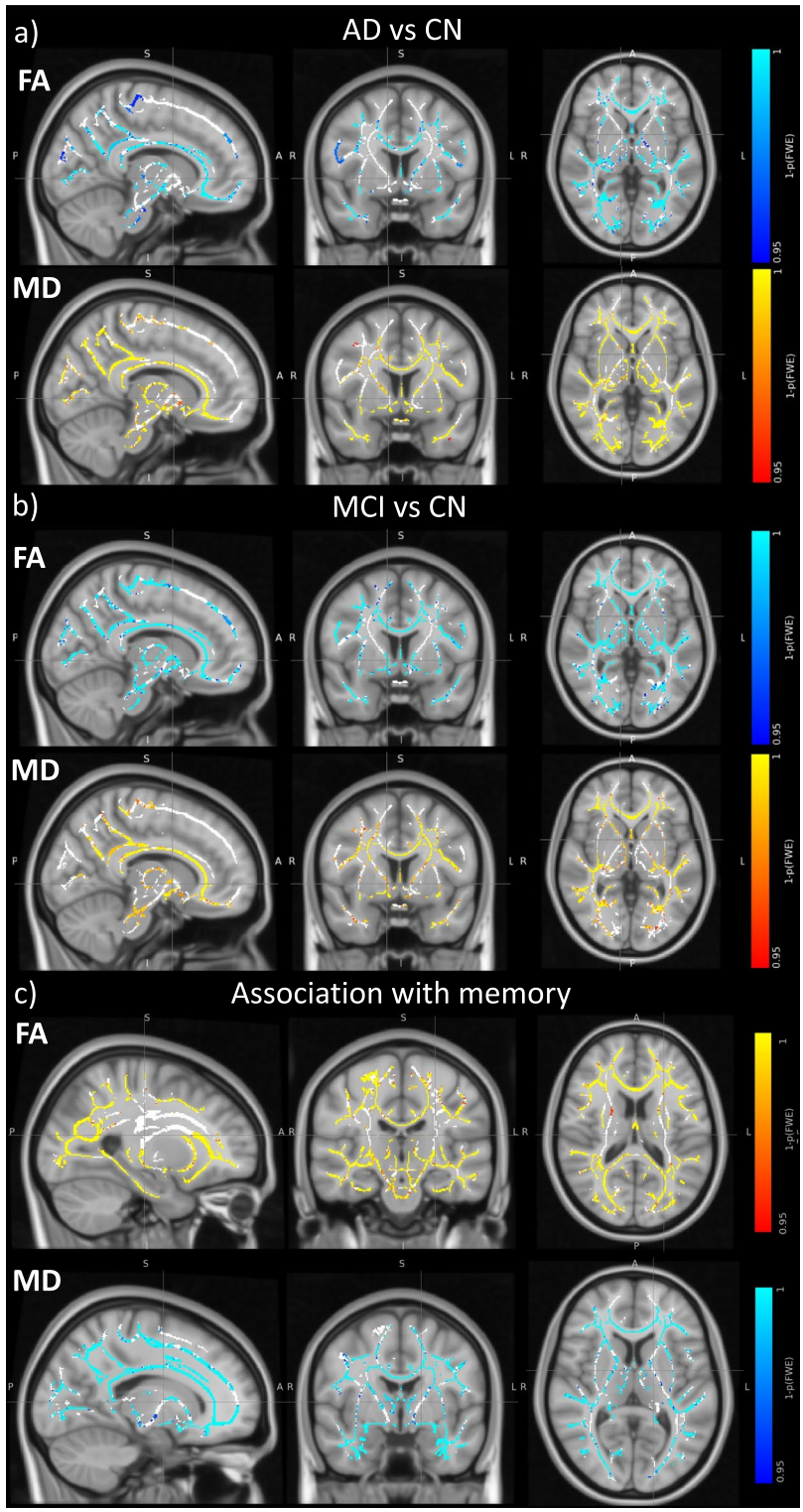

Fig. 5 Differences in tensor-derived measures across controls and clinical subgroups and association with memory. *Note*. AD, Alzheimer's disease; CN, cognitively normal; MCI, mild cognitive impairment; FA, fractional anisotropy; MD, mean diffusivity. The white matter skeleton (white) is plotted on the MNI152 standard space. Tracts associated with memory at $p_{FWE} < .05$ are coloured: **a** and **b** red-to-yellow for significant increase and dark-to-light blue for significant decrease compared to controls **c** red-to-yellow for significantly positive FA association and dark-to-light blue for significantly negative MD association

Discussion

This study made use of FBA to investigate cerebral WM across the age-related neurocognitive spectrum, at the level of neural fibre populations crossing through brain image voxels (fixels), providing a more accurate assessment of the crossing fibre tracts' structure [4, 5, 7]. Specifically, this study analysed the apparent density of neural population fibres, the macrostructure of fibre-bundle cross-sections, and a combined measure of the two previous features [7], and tested their statistical associations with memory performance in the neurocognitive aging spectrum.

Compared to controls, both AD and MCI had reduced FD and FDC in the fornix and fibres extending from the fornix to the MTL, which overlaps with previous AD and MCI FBA studies [5, 10, 11], and may reflect a disease progress (with higher effect size in AD). The FBA results also contrast with previous analyses variously finding reductions in the CC, the cingulum, the inferior longitudinal, inferior fronto-occipital, arcuate, and/or uncinate fasciculi in AD [5, 9, 10], cingular, uncinate, anterior thalamic radiation, and/or forceps minor reductions in MCI [5, 9, 14]. Whilst this raises the question of how robust such findings are, differences across protocols may explain the differences, including separating late and early onset AD [10], using multi-shell DWI images [5, 9, 14], segmentations of tracts of interest [5] and variation in sample size. Whilst the FC reduction in cortico-spinal tract and AC has also been previously reported [5, 9], this is the first observation of a FC increase in AD to our knowledge. Increased FC concomitant with reduced FD has been found in other neurodegenerative diseases, affecting the fornix in Huntington's disease [37], and the tapetum in Parkinson's disease [38]. Whilst there is no definite interpretation, increased cross-section could be the result of extra-axonal aggregates (inter-axonal space filled with cells related to inflammation or gliosis, instead of simply healthy axons (Raffelt et al., 2017)), and a possible partial volume effect (due to the CSF in the lateral ventricles) is discussed later in the discussion.

The FBA and memory analysis showed different patterns across the measures, with log of FC being associated with memory within the AC tract, whilst FD and FDC were mainly associated with memory in the fornix and extending downward fibres in the temporal lobes. These fibres overlap coherently with the MCI and AD subgroups' differences to controls, and especially correspond to changes in the AD group. Fornical WM being associated with memory is consistent with previous DTI findings associating memory with decreased WM in the fornix (lower FA and MD) [39]. This also confirms an FBA study in normal aging where FD in the fornix (and not FC) was specifically investigated and significantly correlated with RAVLT's delay score [15]. The fornix may therefore be linked to cognitive decline in neurocognitive aging, but more precisely drive by its microstructural deterioration (FD) rather than its macrostructural aspect (FC). Associations in the MTL can also be linked to conventional DTI findings of disrupted WM microstructure in the parahippocampal cingulum [40, 41] and a previous FBA study specifically associating various FBA metrics (i.e., FC, FC, and FDC) in the parahippocampal and hippocampal regions with RAVLT's ten-word delayed recall test scores in a MCI sample [14]. However, the associations with memory in the present study are mostly driven by the microstructural features (significant findings only for FD and FDC), but not FC.

Cross-sectional macrostructure of the AC may also explain some variability in memory scores. FDC only overlapped in a fraction of anterior fixels, possibly due to the AC effect being predominantly driven by FC, as FDC combines the variance of each source [7]. AC macrostructure's role in memory performance is unclear, but two conventional DTI studies observed neural (streamline-based) connectivity between the anterior fornix body and regions supporting memory functions in the MTL, through the AC, as a compensatory mechanism for brain injury [42–44]. AC may also be sensitive to neurodegeneration, as suggested by an FBA study showing higher AC FC in AD beta amyloid negative patients compared to AD beta amyloid positive patients [12], and reduced FC and FDC in lateral parts of the AC in another AD cohort [5].

Fixels with significant FD and FDC were also present along the ventricles, which is hard to interpret. Similar patterns can be seen in previous whole-brain MCI and AD-related results [5, 10, 11]. There is a possibility that noise at low b-values in the present study led to spurious estimated WM response function in voxels where CSF and WM are adjacent due to partial volume effect [9, 25]. Furthermore, the associations may also be driven by differences in ventricle and/or hippocampal morphology across the

subgroups. In the presents results, the thin layer of FD fixels longing the posterior surfaces of the lateral ventricles, in the posterior CC, do not extend across the width of the callosal tract, which suggests it could be spurious. These fibre patterns should thus be interpreted with caution.

Tensor-derived measures showed more widespread alterations in AD and MCI, affecting tracts that were not significantly different in the FBA, such as the cingulum bundle, most of the CC, the inferior longitudinal fasciculi and striato-parietal/occipital radiations. Tensor-derived metrics were widely associated with the memory score, affecting almost all WM tracts. Greater WM microstructural integrity (as estimated by increased FA or decreased MD) was associated with better memory performance. This global pattern likely is driven by disease progression in MCI or AD (and its parallel memory impairment): widespread reductions in WM microstructural integrity (measured with FA and MD) using the same TBSS approach to be similarly observed over 1 year of disease progression in an AD cohort from the ADNI2 dataset [45]. Widespread decreases in voxel-wise measurements of WM microstructural integrity in AD and MCI were also reported in other cohorts compared to controls [9]. Such pattern suggests that tensor-derived metrics may be overly sensitive and lack spatial specificity in relation to memory scores in comparison to fixel-wise metrics.

The main strength of this study relates to the fixel-wise examination of WM architecture and tracts. As revealed by our findings, these fixel-wise metrics provide better anatomical specificity compared to conventional DTI measures, accounting for both microstructural and macrostructural changes in fibres [5]. So far, only one study to our knowledge explored specific cognitive measures [14]. The present study also provides a contrast with conventional DTI measures and reinforces the idea that FBA measures exhibit greater anatomical specificity. Another strength is that the analyses were run on a relatively large sample size which reinforces the reliability of the observed effects.

The study being cross-sectional, it is not possible to establish a temporal pattern between the FBA measures and cognitive impairment, and future studies will benefit from a longitudinal design. Another limitation in the present analyses is that they were done on single-shell diffusion weighted images, which had relatively low b-values at $b = 1000$ s/mm^2, as well as variation in the number of directions. Analysing images with higher b-values and more directions will return more accurate estimations of apparent FD due to a stronger attenuation of the extra-axonal water signals which prevents it from contributing to FD estimation [6]. It is possible that WM microstructure estimated at higher b-values may be more sensitive to cognitive functions [14].

This study used a recently developed fixel-wise approach to investigate fibre-specific measures of WM macrostructure and microstructure associated with memory performance in the neurocognitive aging spectrum. We also compared these metrics across different neurocognitive diagnoses. Generally, we found decreased WM microstructural integrity in the fornix and connected tracts in the bilateral MTL, affecting both groups with AD and MCI. These localised decreases were associated with lower memory scores. In AD, macroscopically reduced fibre-cross section was found in the left AC, a WM tract which was also associated with lower memory. In comparison, the TBSS analyses on tensor derived metrics, revealed a more widespread pattern of WM abnormalities which are associated with memory and neurocognitive diagnoses (i.e., MCI and AD). Overall, the fixel-wise approach exhibited greater anatomical specificity compared to the conventional TBSS approach.

Acknowledgements Alzheimer's Disease Neuroimaging Initiative Consortium

For the full list of investigators that have taken part in the ADNI Consortium, please refer to the list provided by the ADNI Data and Publications Committee (July 2024): https://adni.loni.usc.edu/wp-content/uploads/2024/07/ADNI-Acknowledgement-List_July2024.pdf

Author contribution CB and JY: conceptualization, data curation, methodology, software, validation, writing—review and editing. JY: funding acquisition, project administration, supervision, resources. CB: formal analysis, investigation, writing—original draft.

Funding This work is supported by the Nanyang Assistant Professorship (Award no. 021080–00001) grant. Collection and sharing of the data was funded by the ADNI (National Institutes of Health Grant U01 AG024904) and DOD ADNI (Department of Defense award number W81XWH-12–2-0012). ADNI is funded by the National Institute on Aging, the National Institute of Biomedical Imaging and Bioengineering, and through contributions from: AbbVie, Alzheimer's Association; Alzheimer's Drug Discovery Foundation; Araclon Biotech;

BioClinica, Inc.; Biogen; Bristol-Myers Squibb Company; CereSpir, Inc.; Cogstate; Eisai Inc.; Elan Pharmaceuticals, Inc.; Eli Lilly and Company; EuroImmun; F. Hoffmann-La Roche Ltd and its affiliated company Genentech, Inc.; Fujirebio; GE Healthcare; IXICO Ltd.; Janssen Alzheimer Immunotherapy Research & Development, LLC.; Johnson & Johnson Pharmaceutical Research & Development LLC.; Lumosity; Lundbeck; Merck & Co., Inc.;Meso Scale Diagnostics, LLC.; NeuroRx Research; Neurotrack Technologies; Novartis Pharmaceuticals Corporation; Pfizer Inc.; Piramal Imaging; Servier; Takeda Pharmaceutical Company; and Transition Therapeutics. ADNI clinical sites in Canada receives supporting funds from The Canadian Institutes of Health Research. The Foundation for the National Institutes of Health (www.fnih.org) facilitated private sector contributions. The grantee is the "Northern California Institute for Research and Education", whilst the study coordinator is the "Alzheimer's Therapeutic Research Institute at the University of Southern California". The data is disseminated by the Laboratory for Neuro Imaging at the University of Southern California.

Data availability The dataset analysed in the present study is available in the ADNI repository and subject to Data Sharing and Publication Policy: https://adni.loni.usc.edu/wp-content/uploads/how_to_apply/ADNI_DSP_Policy.pdf.

Declarations

Competing interests The authors declare no competing interests.

References

1. Sexton CE, Kalu UG, Filippini N, Mackay CE, Ebmeier KP. A meta-analysis of diffusion tensor imaging in mild cognitive impairment and Alzheimer's disease. Neurobiol Aging. 2011;32(12):2322-e5. https://doi.org/10.1016/j.neurobiolaging.2010.05.019.
2. Yu J, Lam CLM, Lee TMC. White matter microstructural abnormalities in amnestic mild cognitive impairment: a meta-analysis of whole-brain and ROI-based studies. Neurosci Biobehav Rev. 2017;83:405–16. https://doi.org/10.1016/j.neubiorev.2017.10.026.
3. Le Bihan D. Looking into the functional architecture of the brain with diffusion MRI. Nat Rev Neurosci. 2003;4(6):469–80. https://doi.org/10.1038/nrn1119.
4. Jeurissen B, Leemans A, Tournier J, Jones DK, Sijbers J. Investigating the prevalence of complex fiber configurations in white matter tissue with diffusion magnetic resonance imaging. Hum Brain Mapp. 2013;34(11):2747–66. https://doi.org/10.1002/hbm.22099.
5. Mito R, et al. Fibre-specific white matter reductions in Alzheimer's disease and mild cognitive impairment. Brain. 2018;141(3):888–902. https://doi.org/10.1093/brain/awx355.
6. Dhollander T, et al. Fixel-based analysis of diffusion MRI: methods, applications, challenges and opportunities. Neuroimage. 2021;241:118417. https://doi.org/10.1016/j.neuroimage.2021.118417.
7. Raffelt DA, et al. Investigating white matter fibre density and morphology using fixel-based analysis. Neuroimage. 2017;144:58–73. https://doi.org/10.1016/j.neuroimage.2016.09.029.
8. Raffelt DA, et al. Apparent fibre density: a novel measure for the analysis of diffusion-weighted magnetic resonance images. Neuroimage. 2012;59(4):3976–94. https://doi.org/10.1016/j.neuroimage.2011.10.045.
9. Giraldo DL, et al. Investigating tissue-specific abnormalities in Alzheimer's disease with multi-shell diffusion MRI. J Alzheimers Dis. 2022;90(4):1771–91. https://doi.org/10.3233/JAD-220551.
10. Luo X, et al. Distinct fiber-specific white matter reductions pattern in early-and late-onset Alzheimer's disease. Aging. 2021;13(9):12410. https://doi.org/10.18632/aging.202702.
11. Bhattarai A, Maillard P, Decarli C, Fan A. Fixel based analysis of white matter alterations in mild cognitive impairment and Alzheimer's disease. Alzheimers Dement. 2023;19:e079454. https://doi.org/10.1002/alz.079454.
12. Dewenter A, et al. Disentangling the effects of Alzheimer's and small vessel disease on white matter fibre tracts. Brain. 2023;146(2):678–89. https://doi.org/10.1093/brain/awac265.
13. Wang J, Wen C, Li J, Chen J, Feng Y. Automated quantification of brain connectivity in Alzheimer's disease using ClusterMetric. Neurosci Lett. 2022;785:136724. https://doi.org/10.1016/j.neulet.2022.136724.
14. Ahmadi K et al. Fixel-based analysis reveals tau-related white matter changes in early stages of Alzheimer's disease. J Neurosci. 2024;44(18):e0538232024. https://doi.org/10.1523/JNEUROSCI.0538-23.2024.
15. Radhakrishnan H, Stark SM, Stark CE. Microstructural alterations in hippocampal subfields mediate age-related memory decline in humans. Front Aging Neurosci. 2020;12:94. https://doi.org/10.3389/fnagi.2020.00094.
16. Radhakrishnan V, et al. Cerebellar and basal ganglia structural connections in humans: effect of aging and relation with memory and learning. Front Aging Neurosci. 2023;15:1019239. https://doi.org/10.3389/fnagi.2023.1019239.
17. Weiner MW, et al. The Alzheimer's Disease Neuroimaging Initiative 3: continued innovation for clinical trial improvement. Alzheimers Dement. 2017;13(5):561–71. https://doi.org/10.1016/j.jalz.2016.10.006.
18. van der Elst W, van Boxtel MPJ, van Breukelen GJP, Jolles J. Rey's verbal learning test: normative data for 1855 healthy participants aged 24–81 years and the influence of age, sex, education, and mode of presentation. J Int Neuropsychol Soc JINS. 2005;11(3):290–302. https://doi.org/10.1017/S1355617705050344.
19. Dhollander T, Connelly A. A novel iterative approach to reap the benefits of multi-tissue CSD from just single-shell (+ b= 0) diffusion MRI data. Proc 24th Annu Meet Int Soc Magn Reson Med. 2016;24:3010.
20. Tournier J-D, et al. MRtrix3: A fast, flexible and open software framework for medical image processing and visualisation. Neuroimage. 2019;202:116137. https://doi.org/10.1016/j.neuroimage.2019.116137.
21. Veraart J, Novikov DS, Christiaens D, Ades-aron B, Sijbers J, Fieremans E. Denoising of diffusion MRI using

random matrix theory. Neuroimage. 2016;142:394–406. https://doi.org/10.1016/j.neuroimage.2016.08.016.
22. Kellner E, Dhital B, Kiselev VG, Reisert M. Gibbs-ringing artifact removal based on local subvoxel-shifts. Magn Reson Med. 2016;76(5):1574–81. https://doi.org/10.1002/mrm.26054.
23. Tustison NJ, et al. N4ITK: Improved N3 Bias Correction. IEEE Trans Med Imaging. 2010;29(6):1310–20. https://doi.org/10.1109/TMI.2010.2046908.
24. Dhollander T, Mito R, Raffelt D, Connelly A. Improved white matter response function estimation for 3-tissue constrained spherical deconvolution. Proc Intl Soc Mag Reson Med. 2019;27:555. Retrieved from https://archive.ismrm.org/2019/0555.html. Accessed 10 Sept 2024.
25. Jeurissen B, Tournier J-D, Dhollander T, Connelly A, Sijbers J. Multi-tissue constrained spherical deconvolution for improved analysis of multi-shell diffusion MRI data. Neuroimage. 2014;103:411–26. https://doi.org/10.1016/j.neuroimage.2014.07.061.
26. Fischl B. FreeSurfer. Neuroimage. 2012;62(2):774–81. https://doi.org/10.1016/j.neuroimage.2012.01.021.
27. Raffelt DA, et al. Connectivity-based fixel enhancement: whole-brain statistical analysis of diffusion MRI measures in the presence of crossing fibres. Neuroimage. 2015;117:40–55. https://doi.org/10.1016/j.neuroimage.2015.05.039.
28. Smith RE, Tournier J-D, Calamante F, Connelly A. SIFT: spherical-deconvolution informed filtering of tractograms. Neuroimage. 2013;67:298–312. https://doi.org/10.1016/j.neuroimage.2012.11.049.
29. Smith SM, et al. Tract-based spatial statistics: voxelwise analysis of multi-subject diffusion data. Neuroimage. 2006;31(4):1487–505. https://doi.org/10.1016/j.neuroimage.2006.02.024.
30. Smith SM, et al. Advances in functional and structural MR image analysis and implementation as FSL. Neuroimage. 2004;23:S208–19. https://doi.org/10.1016/j.neuroimage.2004.07.051.
31. Rosseel Y. lavaan: an R package for structural equation modeling. J Stat Softw. 2012;48:1–36. https://doi.org/10.18637/JSS.V048.I02.
32. R Core Team. R: a language and environment for statistical computing'. Vienna: R Foundation for Statistical Computing; 2023. [Online]. Available: https://www.r-project.org/. Accessed 29 Aug 2024
33. Smith RE, Dhollander T, Connelly A. 'On the regression of intracranial volume in fixel-based analysis. 27th Int Soc Magn Reson Med. 2019;27:3385.
34. Buckner RL, et al. A unified approach for morphometric and functional data analysis in young, old, and demented adults using automated atlas-based head size normalization: reliability and validation against manual measurement of total intracranial volume. Neuroimage. 2004;23(2):724–38. https://doi.org/10.1016/j.neuroimage.2004.06.018.
35. Winkler AM, Ridgway GR, Webster MA, Smith SM, Nichols TE. Permutation inference for the general linear model. Neuroimage. 2014;92:381–97. https://doi.org/10.1016/j.neuroimage.2014.01.060.
36. Brandmaier AM. onyxR: interface to call Onyx from R. 2018. [Online]. Available: https://rdrr.io/github/brandmaier/onyxR/
37. Oh SL, et al. Fixel-based analysis effectively identifies white matter tract degeneration in Huntington's disease. Front Neurosci. 2021;15:711651. https://doi.org/10.3389/fnins.2021.711651.
38. Rau Y-A, et al. A longitudinal fixel-based analysis of white matter alterations in patients with Parkinson's disease. NeuroImage Clin. 2019;24:102098. https://doi.org/10.1016/j.nicl.2019.102098.
39. Yu J, Lee TM, Alzheimer's Disease Neuroimaging Initiative. Verbal memory and hippocampal volume predict subsequent fornix microstructure in those at risk for Alzheimer's disease. Brain Imaging Behav. 2020;14:2311–22. https://doi.org/10.1007/s11682-019-00183-8.
40. Weiler M, de Campos BM, Nogueira MH, Damasceno BP, Cendes F, Balthazar ML. Structural connectivity of the default mode network and cognition in Alzheimer' s disease. Psychiatry Res Neuroimaging. 2014;223(1):15–22. https://doi.org/10.1016/j.pscychresns.2014.04.008.
41. Wen Q, et al. White matter alterations in early-stage Alzheimer's disease: a tract-specific study. Alzheimers Dement Diagn Assess Dis Monit. 2019;11:576–87. https://doi.org/10.1016/j.dadm.2019.06.003.
42. Jang SH, Kwon HG. Perspectives on the neural connectivity of the fornix in the human brain. Neural Regen Res. 2014;9(15):1434. https://doi.org/10.4103/1673-5374.139459.
43. Jang SH, Kwon HG. Neural connectivity of the anterior body of the fornix in the human brain: diffusion tensor imaging study. Neurosci Lett. 2014;559:72–5. https://doi.org/10.1016/j.neulet.2013.06.017.
44. Yeo SS, Jang SH. Neural reorganization following bilateral injury of the fornix crus in a patient with traumatic brain injury. J Rehabil Med. 2013;45(6):595–8. https://doi.org/10.2340/16501977-1145.
45. Mayo CD, Mazerolle EL, Ritchie L, Fisk JD, Gawryluk JR. Longitudinal changes in microstructural white matter metrics in Alzheimer's disease. NeuroImage Clin. 2017;13:330–8. https://doi.org/10.1016/j.nicl.2016.12.012.